Fundamental Insulation Characteristics of High-Pressure CO_2 Gas for Gas-Insulated Power Equipment

- Effect of Coating Conductor on Insulation Performance and Effect of Decomposition Products on Creeping Insulation of Spacer -

Hisashi Goshima
Electric Power Apparatus Insulation Sector, Electric Power Engineering Research Laboratory,
Central Research Institute of Electric Power Industry
2-6-1 Nagasaka, Yokosuka, 240-0196, Japan

Shigemitsu Okabe
Tokyo Electric Power Company
4-1 Egasaki-cho, Tsurumi-ku, Yokohama, 230-8510, Japan

Toshiaki Ueda
Chubu Electric Power Company
20-1Kitasekiyama, Ohdaka-cho, Nagoya, 459-8522, Japan

Hiroshi Morii
Kansai Electric Power Company
3-11-20 Nakoji, Amagasaki, 661-0974, Japan

Nobuhiko Yamachi
Hokuriku Electric Power Company
15-1 Ushijima-Cho, Toyama, 930-8686, Japan

Koji Takahata
Shikoku Electric Power Company
2-5 Marunouchi, Takamatsu, 760-8573, Japan

and **Masayuki Hikita**
Kyushu Institute of Technology
1-1Sensui-cho, Tobata, Kitakyushu, 840-8550, Japan

ABSTRACT

Currently, environmental problems such as global warming are important issues, and SF_6 has been identified as a greenhouse gas with a long atmospheric lifetime. Therefore, in the long term, it is preferable to reduce the amount of SF_6 used as an insulating gas. It is thus important to discuss the possibility of using more environmentally friendly gases as alternative insulation for gas-insulated apparatus. In this paper, we describe the fundamental insulation breakdown characteristics of high-pressure CO_2 gas at gas pressures of up to 1.0 MPa under simulated practical conditions, including the insulation breakdown characteristics of a high-voltage conductor with an insulating coating and the effect of decomposition products on the creeping insulation of a spacer. With the aim of enhancing insulation performance, we discuss the effect of the type of insulating coating on insulation performance. The breakdown electric field was increased by 20% by coating the conductor. It was verified that the application of an insulating coating is a practical method for enhancing the insulation performance of high-pressure CO_2 gas. It was also verified that the decomposition products have only a slight effect on the creeping insulation of the spacer except for when there is heavy pollution on the insulating spacer. However, if a large amount of decomposition products is expected to be deposited on the insulating spacer during operation, which may cause a severe interruption to the current, it will be necessary to consider this factor in the insulation design.

Index Terms —**Insulating gas, SF_6 substitute, CO_2 gas, gas-insulated switchgear (GIS), insulation breakdown characteristics, electrode coating, decomposition products.**

1 INTRODUCTION

BECAUSE of its excellent insulation and interruption performance, SF_6 has been applied to gas-insulated switchgear (GIS), gas-blast circuit breaker (GCB), and gas-insulated transmission line (GIL) and has contributed to the miniaturization of equipment and the achievement of high performance. Currently, environmental problems such as global warming are important issues, and SF_6 has been identified as a greenhouse gas with a long atmospheric lifetime [1]. Therefore, recycling guidelines for SF_6 in electric power equipment have been examined, and a reduction in the

Manuscript received on 11 October 2007, in final form 8 February 2008.

amount of SF_6 released into the atmosphere has been targeted [2-5]. In the long term, it is preferable to reduce the amount of SF_6 used as an insulation gas. Therefore, it is important to discuss the possibility of using more environmentally friendly gases as alternative insulation for gas-insulated apparatus [6-10]. Meanwhile, the number of gas-insulated apparatus more than 30 years old is increasing because a large number of these apparatus have been installed since the 1970s. Therefore, it is requested that the aged apparatus should be used to their utmost limit by postponing their replacement to as late a date as possible. Moreover, regarding the replacement of apparatus, it is important to examine the switchover to more environmentally friendly apparatus by assessing the life cycle cost and performance.

In the selection of an alternative, more environmentally friendly gas, it is thought that high-pressure natural gases, such as air, nitrogen (N_2), and carbon dioxide (CO_2), are promising candidates. In this study, we considered the use of high-pressure CO_2 gas. We have previously investigated the fundamental insulation characteristics (the insulation breakdown characteristics under a clean condition for a lightning impulse and ac voltage, and the breakdown characteristics when metallic particles are deposited on the central conductor and insulating spacer surface) at high pressures of up to 2.0 MPa [11]. As a result, it was verified that the condition of the high-voltage-conductor surface had a strong effect on the insulation breakdown characteristics of high-pressure CO_2. Moreover, it is desirable that some strategies are given for enhancing the insulation performance of apparatus using CO_2 insulation because such apparatus require a larger size and a higher gas pressure than current SF_6-insulated apparatus. From this viewpoint, we examined the insulation breakdown characteristics of a high-voltage conductor with an insulating coating.

On the other hand, a large amount of decomposition products was generated during current-interrupting tests of CO_2 gas using a 72 kV-class GCB. Moreover, a decrease in the insulation resistance between the conductor and the grounding tank occurred when CO_2 gas was replaced with air upon opening the test tank after the current-interrupting tests. Therefore, there is concern that the decomposition products may affect the insulation performance of solid insulators, such as the insulating spacer. Thus, we also investigated the effect of the decomposition products on the creeping insulation of a spacer.

2 BREAKDOWN CHARACTERISTICS OF CONDUCTOR WITH INSULATING COATING

In this chapter, we report the experimental evaluation of the insulation breakdown characteristics of a high-voltage conductor with various insulating coatings upon the application of a lightning impulse (LI) voltage with the aim of enhancing insulation performance.

2.1 EXPERIMENTAL SETUP AND PROCEDURE

A coaxial cylindrical electrode for a single-phase bus line used for 72 kV-class GIS was tested. Figure 1 shows the structure of the coaxial cylindrical electrode, and Figure 2 shows a photograph of the installed electrode. The central conductor applying the high voltage was 70 mm in diameter, while the diameter of the grounding sheath electrode was 150 mm; the gap length was thus 40 mm. The electric field utilization factor was 0.67. Both electrodes were made of aluminum. The CO_2 gas pressures were set at 0.4, 0.7, and 1.0 MPa.

The surface condition of the central conductor was utilized as a parameter to discuss the improvement of insulation breakdown characteristics under impulse voltage. Table 1 shows the different surface conditions of the central conductor. Condition 1 (hereafter, referred to as Bare-1) was a bare electrode (standard condition). The surface roughness was 25 μm. Condition 2 (hereafter, Bare-2) was also a bare electrode but with a surface roughness of 10 μm. Conditions 3 (Anodic Oxide) and 4 (TUFRAM®) were central conductors treated with an anodic oxide coating on the aluminum conductor. TUFRAM® is a technique of forming a hard anodic oxide coating on aluminum by immersion in PTFE. Conditions 5 (Fluorine-1) and 6 (Fluorine-2) were fluorine (PFA and PTFA)-coated conductors, and the thicknesses of the coatings were approximately 60 μm and 400 μm, respectively. Condition 7 (Epoxy) was an epoxy-resin-coated conductor (approximately 500 μm thick). Note that the surface roughness of electrode before coating was same to Bare-1.

Standard positive and negative LIs were applied by the step-up method, and the 50% breakdown voltage and its

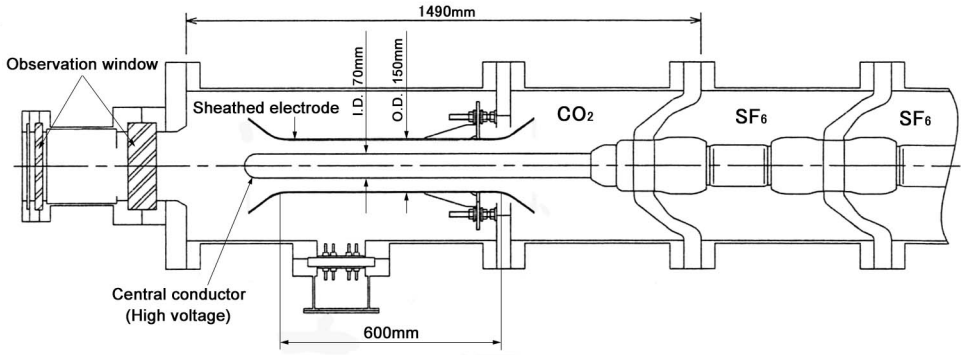

Figure 1. Coaxial cylindrical test electrode of 72 kV-class GIS.

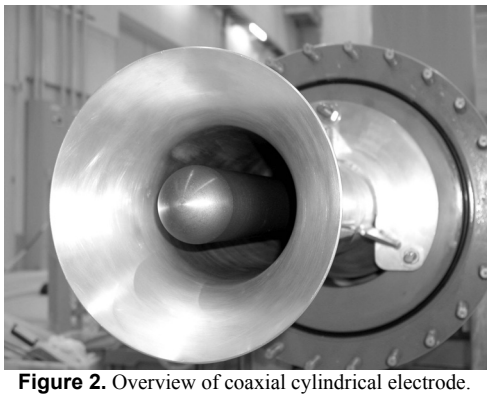

Figure 2. Overview of coaxial cylindrical electrode.

Table 1 Surface conditions of central conductor (high-voltage electrode).

Name	Surface condition
#1: Bare-1	Bare electrode (surface roughness: 25 μm)
#2: Bare-2	Bare electrode (surface roughness: 10 μm)
#3: Anodic oxide	Anodic oxide coating on aluminum
#4: TUFRAM®	TUFRAM® (Hard anodic oxide coating & immersion of PTFE)
#5: Fluorine-1	Fluorine (PFA; Tetrafluoroethylene-perfluoroalkylvinyl ether copolymer & PTFE; polytetrafluoroethylene) coating (thickness: 60 μm)
#6: Fluorine-2	Fluorine (PFA & PTFE) coating (thickness: 400 μm)
#7: Epoxy	Epoxy resin coating (thickness: 500 μm)

variation were estimated by statistical analysis of the Weibull distribution. The discharge state was filmed from the observation window using a still camera.

2.2 EFFECT OF ELECTRODE SURFACE ROUGHNESS OF BARE ELECTRODE

Figure 3 shows Weibull plots of the insulation breakdown electric field (BDE) on the central conductor surface for a negative LI at a gas pressure of 1.0 MPa for Bare-1 and Bare-2. The 50% BDE E_{50} of Bare-2 was approximately 13% higher than that of Bare-1. Smoothing the electrode surface increased E_{50} by approximately 14% for the application of a given ac voltage [11]. The shape parameters of the Weibull distributions were 40 for Bare-1 and 46 for Bare-2, and the variations of BDE were small (with a standard deviation of approximately 3%). From these results, it was verified that E_{50} was increased by at least 10% by smoothing the conductor surface.

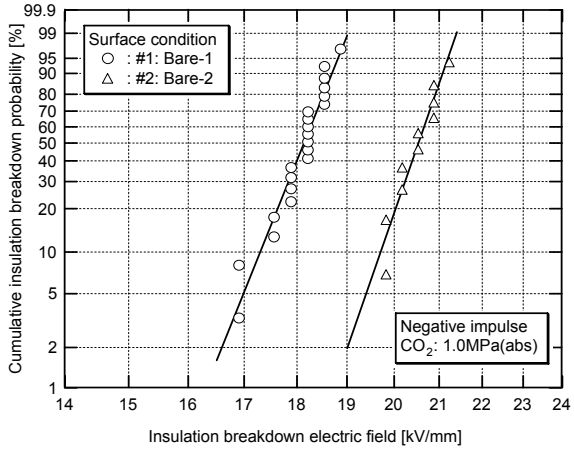

Figure 3. Weibull plots of insulation BDE for negative LI for Bare-1 and Bare-2 (CO_2: 1.0 MPa (abs)).

2.3 EFFECT OF CONDUCTOR COATING

Figure 4 shows BDE for a negative LI as a function of experiment number for different electrode surface conditions, and Table 2 summarizes the state of the discharge for the different electrode surface coatings. Moreover, Figure 5 shows Weibull plots of BDE for the different surface coatings of the electrodes. For Anodic Oxide, discharge points (breakdown traces) were random. Some values of BDE for Anodic Oxide were very low and were similar to those for Bare-1, as shown in Figure 4. Discharge points for TUFRAM® were also random, and the values of BDE were very stable and high. Figure 6 shows a comparison of BDE (E_{50} estimated from Figure 5 and the first BDE shown in

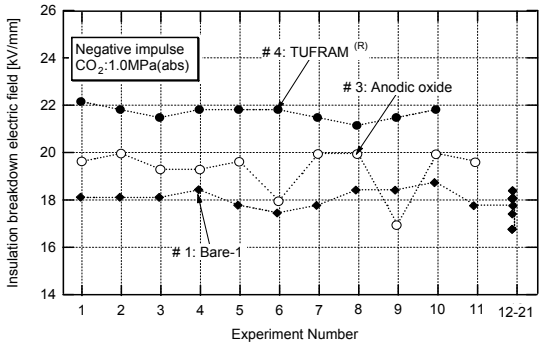

(a) #3 and #4

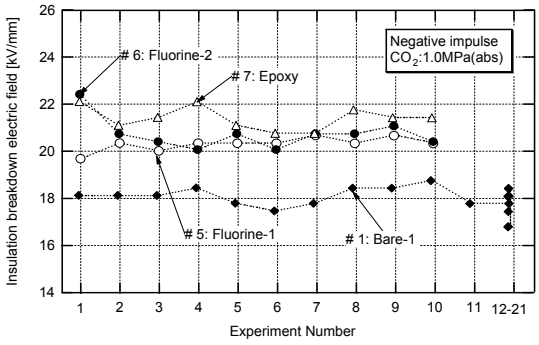

(b) #5 - #7

Figure 4. Insulation BDE for negative LI as a function of experiment number for different electrode surface conditions (CO_2: 1.0 MPa (abs)).

Table 2 State of discharge for different electrode surface conditions.

Name	State of discharge (10 times)
#3: Anodic oxide	Discharge points are random. Some values of BDE are very low.
#4: TUFRAM®	Discharge points are random. The values of BDE are very stable.
#5: Fluorine-1	Discharge points are random. The values of BDE are very stable.
#6: Fluorine-2	Discharge concentrated at three points (near each other). First BDE is high.
#7: Epoxy	Discharge concentrated at two points.

Figure 4) between Bare-1 and the coated electrodes. For TUFRAM®, both E_{50} and the first BDE were more than 20% higher than those of Bare-1.

For Fluorine-1, the discharge points and the variation of BDE were similar to those for TUFRAM®. However, the values of BDE for Fluorine-1 were lower than those for TUFRAM®. As shown in Figure 6, the first BDE of Fluorine-2 was higher than that of Fluorine-1 since the coating was thicker. However, from the second breakdown, the values of BDE for Fluorine-2 were lower than that of the first BDE. Consequently, E_{50} for Fluorine-2 was similar to that for Fluorine-1 and the discharge trace was concentrated at three points very near to each other in this experiment. For Epoxy, the discharge trace was concentrated at two points. Thus, the breakdown trace tended to be concentrated at a number of points, and the first BDE was higher than subsequent BDEs when the coating was comparatively thick (several hundred μm).

The value of the first BDE is an important factor in the application of an insulating coating to equipment. From this viewpoint, coating the conductor with TUFRAM®, Fluorine-2, or Epoxy is expected to improve BDE. On the other hand, from the viewpoint of manufacturing, the thicker the insulating coating (in the cases of Fluorine-2 and Epoxy), the greater the probability of defects, which become weak points resulting in discharge. However, TUFRAM® coatings have been applied in many industries. The TUFRAM® process produces a hard anodic oxide coating on aluminum, with its voids removed by immersion in PTFE. Therefore, it is expected that there are few defects that may result in discharge in the coating. Thus, we judged that TUFRAM® was the best coating out of the five types of insulating coating considered.

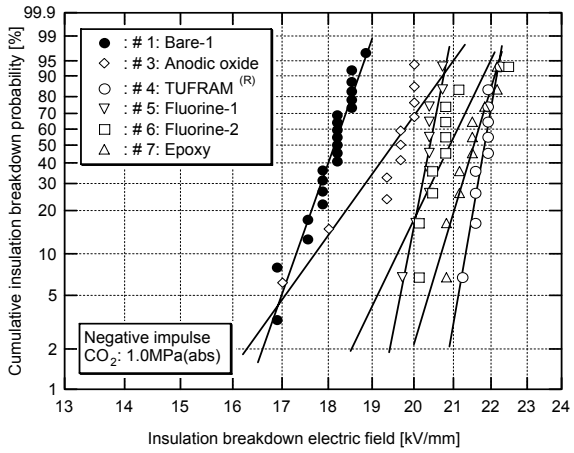

Figure 5. Weibull plots of insulation BDE for different surface coatings of electrodes (CO_2: 1.0 MPa (abs)).

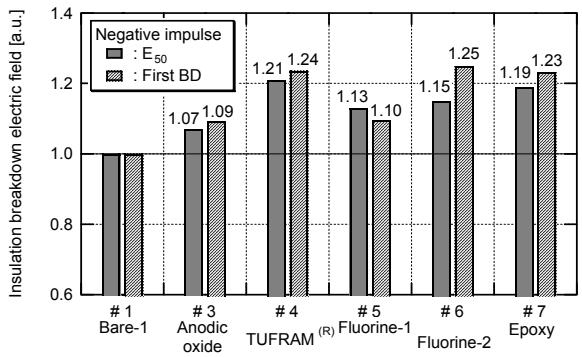

Figure 6. Comparison of insulation BDE between bare and coated electrodes (CO_2: 1.0 MPa (abs)).

2.4 INSULATION BREAKDOWN CHARACTERISTICS USING TUFRAM® COATING

As mentioned above, it was demonstrated that TUFRAM® was the best coating in our experiment. Therefore, in this section, we limit the surface coating to TUFRAM®, and discuss the polarity effect and gas pressure dependence of E_{50}.

2.4.1 POLARITY EFFECT

We previously examined BDE for a negative LI because the insulation design used for the central conductor is determined by the negative LI [11]. To confirm whether this is also valid for a TUFRAM® coating, we also obtained BDE for a positive LI. Figure 7 shows Weibull plots of BDE for a positive and negative LIs for TUFRAM® and Bare-1. It can be seen from this figure that BDE for the negative LI for TUFRAM® was lower than that for the positive LI, the same as for Bare-1. Therefore, it was verified that the insulation design used for the central conductor with a TUFRAM® coating should also be determined by the negative LI. Note that the positive E_{50} of TUFRAM® was approximately 27% higher than that of Bare-1.

2.4.2 GAS PRESSURE DEPENDENCE

Figure 8 shows 50% BDE E_{50} for a negative LI as a function of gas pressure for Bare-1 and TUFRAM®. The error bars of each marker indicate three standard deviations, 3σ, which were estimated from the shape parameter of the Weibull distribution. Note that the value of $E_{50}(1\text{-}3\sigma)$ corresponds to BDE of approximately 1.3% value. It can be seen from this figure that E_{50} for TUFRAM® increased linearly with gas pressure up to 1.0 MPa and was approximately 20% higher than that for Bare-1.

In Figure 8, the equations obtained by curve fitting based on the least-squares approximation are shown. The equation obtained for E_{50} for TUFRAM® is

$$E_{50} = 22.0 \times P^{0.79} \quad (E_{50}\,[\text{kV/mm}],\ P\,[\text{MPa (abs)}]). \qquad (1)$$

For Bare-1, we previously obtained the equation from experimental data up to a gas pressure of 2.0 MPa [11]. In this paper, the equation obtained from data up to a gas pressure of 1.0 MPa for Bare-1 is

$$E_{50} = 18.1 \times P^{0.84} \quad (E_{50}\,[\text{kV/mm}],\ P\,[\text{MPa (abs)}]). \qquad (2)$$

E_{50} increases linearly with the 0.79^{th} power of gas pressure for TUFRAM®, and with the 0.84^{th} power for Bare-1. Therefore, it was verified that the gas pressure dependence for TUFRAM® is similar to that of Bare-1; E_{50} was increased by approximately 20% in the range of gas pressures from 0.4 to 1.0 MPa by coating the conductor with TUFRAM®

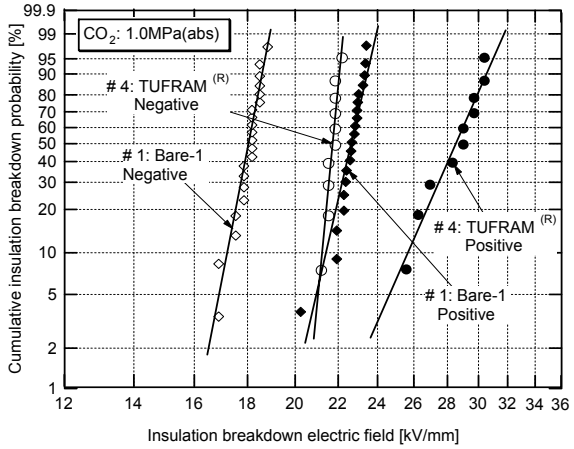

Figure 7. Weibull plots of insulation BDE for TUFRAM®-coated electrode (CO_2: 1.0 MPa (abs)).

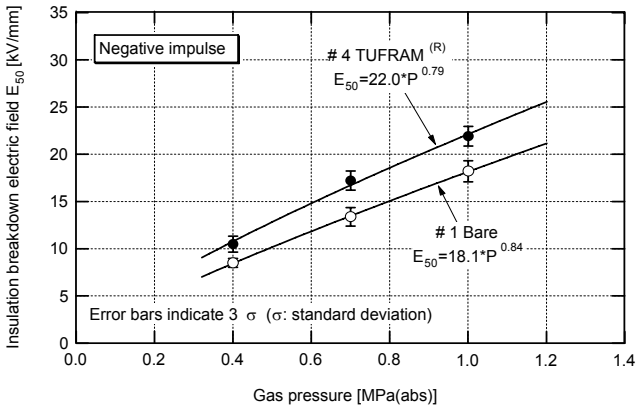

Figure 8. Insulation BDE E_{50} for negative LI as a function of gas pressure for Bare-1 and TUFRAM®.

3 BREAKDOWN CHARACTERISTICS WITH DECOMPOSITION PRODUCTS ON INSULATING SPACER

As mentioned previously, a large amount of decomposition products was generated during the current-interrupting tests of CO_2 gas using the 72 kV-class GCB, and a decrease in the insulation resistance occurred when CO_2 gas was replaced with air upon opening the test tank after the current-interrupting tests. Therefore, in this section, we report the experimental evaluation of the effect of the decomposition products on the creeping insulation of a spacer.

3.1 EXPERIMENTAL SETUP AND PROCEDURE

Figure 9 shows the coaxial cylindrical test electrode including the insulating spacer (spacer model). The insulating spacer was a cone-type model and was made of epoxy resin with alumina filler, the same as that used in current SF_6 insulation apparatus. The material of the central conductor and the sheathed electrode was aluminum. The decomposition products were obtained from the current-interrupting tests of CO_2 gas using the 72 kV-class GCB. The main constituents were CuF_2, WO_2, WO_3, $Cu_{0.4}W_{0.6}$, AgF_2, and $Cu(OH)_2 \cdot H_2O$.

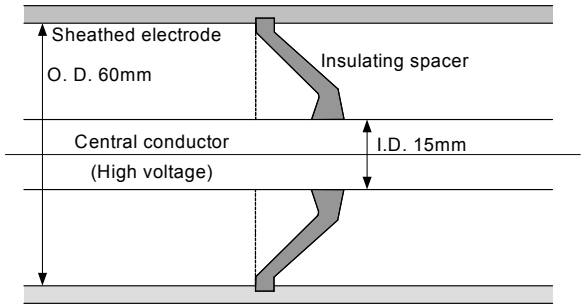

Figure 9. Coaxial cylindrical test electrode including insulating spacer (spacer model).

The decomposition products were spread over the insulating spacer surface by hand, and the insulating spacer was installed in the previously described testing tank. Although it was difficult to quantitatively estimate the amount of decomposition products on the insulating spacer surface, three levels of pollution were set up, as described in Section 3.3. A clean condition (no decomposition products) was also set up. The gas pressure of CO_2 was set at 1.0 MPa.

Standard positive and negative LIs were each applied ten times by the step-up method, and the 50% breakdown voltage and its variation were estimated by statistical analysis of the Weibull distribution. The discharge state was filmed from the observation window using a still camera, although we could only observe the discharge on the concave side of the insulating spacer because of the direction of the observation window. Moreover, we also measured the insulation resistance before the LI test, because we experienced a decrease in the insulation resistance after the current-interrupting test, as mentioned above.

3.2 BREAKDOWN CHARACTERISTICS UNDER CLEAN CONDITION

Figure 10 shows Weibull plots of the breakdown voltage for positive and negative LIs using the spacer model. Under the clean condition, the breakdown mainly occurred in the CO_2 gas for both polarities. The spacer used in this experiment was designed for use with SF_6 gas, and it was not considered that creeping discharge would occur on the spacer.

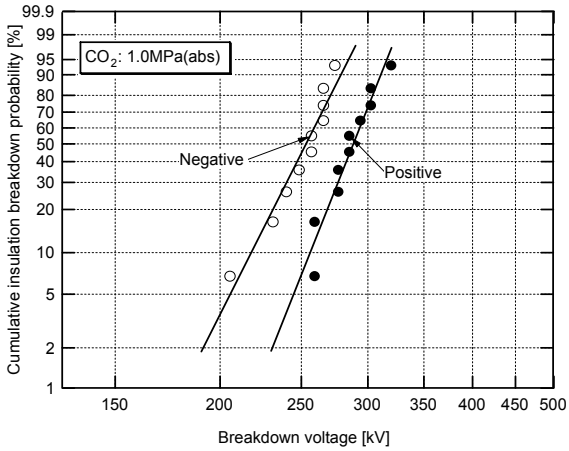

Figure 10. Weibull plots of breakdown voltage using spacer model for different impulse polarities.

(a) Light pollution (b) Medium pollution (c) Heavy pollution

Figure 11. Levels of pollution of decomposition products.

Because the breakdown using the spacer in CO_2 gas occurred without creeping discharge on the spacer, we may be able to use the design of the insulating spacer for SF_6-gas-insulated apparatus as a basis for the insulating spacer for apparatus using CO_2.

It can be seen from Figure 10 that the breakdown voltage for negative polarity was lower than that for positive polarity, the same as for the results in Section 2. E_{50} on the central conductor surface using the spacer model was approximately 30% higher than that using the coaxial cylindrical electrode, as shown in Figure 3, because the electrode size of the spacer model was small and the surface was smooth compared with those of the coaxial cylindrical electrode.

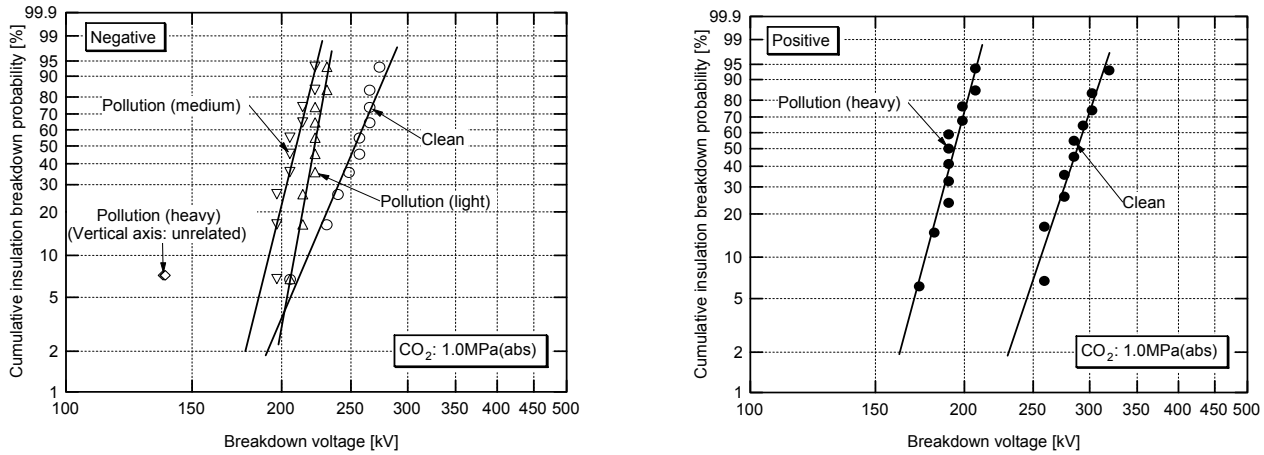

(a) Negative polarity (b) Positive polarity

Figure 12. Weibull plots of breakdown voltage for insulating spacer model with decomposition products.

3.3 INSULATION RESISTANCE OF INSULATING SPACER WITH DECOMPOSITION PRODUCTS

Figure 11 shows the levels of pollution of the decomposition products. Three levels of pollution were set up. Figure 11a shows light pollution, Figure 11b shows medium pollution, and Figure 11c shows heavy pollution. For light and medium pollution, the insulation resistance was its normal value for all the situations of the experiment.

For heavy pollution, the insulation resistance was low (several megaohms) when the spacer model was installed at atmospheric pressure. However, the insulation resistance recovered to its normal value when the test tank was filled with CO_2 gas after the air was removed to form a vacuum. Moreover, the insulation resistance became low again (several tens of megaohms) upon the release of CO_2 gas from the test tank. Thus, for heavy pollution, we observed the same phenomena of the decrease in the insulation resistance as after the current-interrupting test. The insulation resistance recovered in both cases by filling the test tank with CO_2 gas after removing the air. Therefore, the decrease in the insulation resistance may be due to the absorption of moisture by the decomposition products.

3.4 BREAKDOWN CHARACTERISTICS WITH DECOMPOSITION PRODUCTS ON INSULATING SPACER SURFACE

Figures 12a and 12b show Weibull plots of the breakdown voltage for negative and positive polarity, respectively, for the different levels of pollution. Figure 13 shows the breakdown (creeping discharge) traces on the insulating spacer. For light pollution, one creeping discharge (per 10 step-up tests) occurred, as shown in Figure 13a, and two creeping discharge paths (per 10 step-up tests) were observed on the convex side of the insulating spacer for medium pollution. The breakdown voltage for heavy pollution was much lower than that for the

(a) Light pollution (b) Medium pollution (c) Heavy pollution

Figure 13. Breakdown (creeping discharge) traces on insulating spacer.

other cases; we were only able to conduct three tests for heavy pollution because the breakdown voltage became lower than the minimum applied voltage of the impulse generator. In each of these tests, creeping discharge occurred on the concave side of the insulating spacer.

It can be seen from Figure 12a that the 50% breakdown voltages V_{50} for negative polarity with light and medium pollution were approximately 82 to 88% of the values under the clean condition. However, the scattering of the breakdown voltage under low and medium pollution was smaller than that under the clean condition. Therefore, the effect of the decomposition products on the minimum breakdown voltage (for example, 5% breakdown voltage) was slight for light and medium pollution. For heavy pollution, V_{50} for negative polarity was 55% of the value under the clean condition, and the decomposition products had a marked effect.

For the positive polarity, only data for heavy pollution was obtained, as shown in Figure 12b. Six creeping discharge paths (5 paths on the convex side and 1 path on the concave side) were observed on the insulating spacer. V_{50} was approximately 67% of the value under the clean condition, and the effect of the decomposition products under heavy pollution was large, as in the case of negative polarity.

Thus, it was verified that the decomposition products may have only a slight effect on the creeping insulation of the spacer except for when there is heavy pollution of the spacer. However, if a large amount of decomposition products is expected to be deposited on the insulating spacer, which may result in a severe interruption to the current, it will be necessary to consider this factor in the insulation design.

4 CONCLUSION

In this study, we considered the use of high-pressure CO_2 gas as a substitute for SF_6 gas because of its reduced environmental impact. With the aim of providing useful data for rational insulation design, the fundamental insulation breakdown characteristics of high-pressure CO_2 gas for gas pressures of up to 1.0 MPa were acquired under simulated practical conditions. We obtained the insulation breakdown characteristics of a high-voltage conductor with an insulating coating and studied the effect of decomposition products on the creeping insulation of a spacer.

With the aim of enhancing insulation performance, we discussed the effect of the surface roughness of the conductor and the type of insulating coating on the insulation breakdown electric field. E_{50} was increased by approximately 10% by reducing the roughness of the conductor surface. Moreover, E_{50} was increased by approximately 20% in the range of gas pressures from 0.4 to 1.0 MPa by coating the conductor with TUFRAM®. It was verified that an insulating coating such as TUFRAM® should be applied to enhance the insulation performance of high-pressure CO_2 gas.

Regarding the effect of decomposition products on the creeping insulation of a spacer, breakdown under a clean condition was shown to occur without creeping discharge on the spacer. Therefore, we may be able to use the design of the insulating spacer for SF_6-gas-insulated apparatus as a basis for the insulating spacer for apparatus using CO_2. Moreover, it was verified that the decomposition products have only a slight effect on the creeping insulation of the spacer except for when there is heavy pollution of the insulating spacer. However, if a large amount of decomposition products is expected to be deposited on the insulating spacer, which may result in a severe interruption to the current, it will be necessary to consider this factor in the insulation design.

ACKNOWLEDGMENT

The authors wish to express their deepest gratitude to Professor H. Okubo of Nagoya University for his instruction, and the staff concerned at Hitachi, Ltd., for their cooperation and helpful comments.

REFERENCES

[1] CIGRE TF01 WG23.10, "SF_6 and the Global Atmosphere", Electra, No.164, 1996.

[2] CIGRE TF01 WG_B3.02, "SF_6 recycling guide -Use of SF_6 gas in electrical power equipment and final disposal", Technical Brochure, No.234, 2003.

[3] Electric Technology Research Association Report in Japan, "Standard of SF_6 handling", Vol. 54, No.3, 1998. (in Japanese)

[4] T. Kawamura, M. Meguro, H. Hama, and T. Yamagiwa, "Industrial Outlook: How to Reduce SF_6 Use and Emission – Various Aggressive Approaches to Realize less SF_6 Environment", Gaseous Dielectrics X, pp.475-484, 2004.

[5] L. G. Christophorou, J. K. Olthoff, and R. J. Van Brunt, "Sulfur Hexafluoride and the Electric Power Industry", IEEE Electr. Insul. Mag., Vol.13, No.5, pp.20-24, 1997.

[6] CIGRE WG 23/21/33-15, "Gas Insulated Transmission Lines (GIL), Appendix B: GIL Insulation Coordination, On-site Test, Long Duration Test, Monitoring and Grounding", Technical Brochure No.218, 2002.
[7] K. Juhre, and E. Kynast, "High pressure N_2, N_2/CO_2 and CO_2 gas insulation in comparison to SF_6 in GIS applications", 14th ISH, C-01, 2005.
[8] N. Hayakawa, J. Deng, and H. Okubo, "Impulse Partial Discharge and Breakdown Characteristics under Non-uniform Electric Field in CO_2 and N_2/CO_2 Gas Mixtures", 13th ISH, p.424, 2003.
[9] T. Uchii, Y. Hoshina, T. Mori, H. Kawano, T. Nakamoto, and H. Mizoguchi, "Investigations on SF_6-free Gas Circuit Breaker Adopting CO_2 Gas As an Alternative Arc-quenching and Insulating Medium", Gaseous Dielectrics X, pp.205-210, 2004.
[10] H. Goshima, H. Shinkai, and H. Fujinami, "Lightning Impulse Breakdown Characteristics of High-Pressure CO_2 Compared with Those of N_2 as Alternative Insulation Gases to SF_6", 13th ISH, p.443, 2003.
[11] S. Okabe, H. Goshima, A. Tanimura, S. Tsuru, Y. Yaegashi, E. Fujie, and H. Okubo, "Fundamental Insulation Characteristics of High-Pressure CO_2 Gas under Actual Equipment Conditions", IEEE Trans. Dielectr.Electr.Insul., Vol.14, pp.83-90, 2007.

Hisashi Goshima was born on 12 September 1969. He received the B.S. and the M.Eng. degrees in electrical engineering and the Ph.D. degree in engineering from Nagoya University, Nagoya, Japan in 1992, 1994, and 1996, respectively. He joined Central Research Institute of Electric Power Industry in 1996. He was a visiting scientist at University of Hannover, Germany from October 2005 to September 2006. He has been engaged in the study of gas insulation technology of power apparatus and electromagnetic field analysis of upward lightning discharge. Dr. Goshima is a member of IEE of Japan.

Shigemitsu Okabe (M'98) was born on 18 September 1958. He received the B. Eng., M.Eng. and Dr. degrees in electrical engineering from the University of Tokyo in 1981, 1983 and 1986, respectively. He has been with Tokyo Electric Power Company since 1986, and presently a group manager of High Voltage & Insulation Group at R & D center. He was a visiting scientist at Technical University of Munich in 1992. He has been involved in several research projects on the electrical insulation of transmission and distribution apparatuses. Dr. Okabe is a member of IEE of Japan.

Toshiaki Ueda was born in Shizuoka Prefecture, Japan, on 18 June 1962. He graduated in 1985 and obtained a Master's degree in 1987 from the Department of Electrical Engineering, Tohoku University. He obtained the Doctor's degree in 1998 from Nagoya University. He joined Chubu Electric Power Co., in 1987 and has been engaged in research on lightning surge analysis of power systems and substation equipment. Dr. Ueda is a senior member of the IEE of Japan.

Hiroshi Morii was born on 30 April 1957. He received the B.Eng. degree fron Doshisya University in 1981. He has been with The Kansai Electric Power Co. Inc. since 1981. Mr. Morii is a member of IEE of Japan.

Nobuhiko Yamachi was born on 25 June 1969. He received the B.Eng and the M.Eng. degrees in electrical engineering from Toyama University in 1993, 1995, respectively. He has been with Hokuriku Electric Power Company in 1995. Mr. Yamachi is a member of IEE of Japan.

Koji Takahata was born on 8 August 1962. He received the B.Eng. and M.Eng. degrees in electrical engineering from Osaka University in 1985 and 1987, respectively. He joined Shikoku Electric Power Co., Inc. in 1987. He has been engaged in construction and maintenance of Transmission and Substation.

Masayuki Hikita (M'97-SM'98) was born in 1953. He received the B.S., M.S., and Dr. degrees in electrical engineering from Nagoya University of Japan, in 1977, 1979, and 1982, respectively. He was an Assistant, a Lecturer, and Associate Professor at Nagoya University in 1982, 1989, and 1992, respectively. Since 1996, he has been a professor of the Department of Electrical Engineering, Kyushu Institute of Technology. He was Visiting Scientist at the High Voltage Laboratory in MIT, USA, from 1985 to 1987. Dr. Hikita has recently been interested in research on development of diagnostic technique of power equipment. He is a member of the Japan Society of Applied Physics.